

# Mimicking the colourful wing scale structure of the *Papilio blumei* butterfly

Mathias Kolle<sup>1,2</sup>, Pedro M. Salgard-Cunha<sup>1</sup>, Maik R. J. Scherer<sup>1</sup>, Fumin Huang<sup>1</sup>, Pete Vukusic<sup>3</sup>, Sumeet Mahajan<sup>1</sup>, Jeremy J. Baumberg<sup>1\*</sup> and Ullrich Steiner<sup>1\*</sup>

**The brightest and most vivid colours in nature arise from the interaction of light with surfaces that exhibit periodic structure on the micro- and nanoscale. In the wings of butterflies, for example, a combination of multilayer interference, optical gratings, photonic crystals and other optical structures gives rise to complex colour mixing. Although the physics of structural colours is well understood, it remains a challenge to create artificial replicas of natural photonic structures<sup>1–3</sup>. Here we use a combination of layer deposition techniques, including colloidal self-assembly, sputtering and atomic layer deposition, to fabricate photonic structures that mimic the colour mixing effect found on the wings of the Indonesian butterfly *Papilio blumei*. We also show that a conceptual variation to the natural structure leads to enhanced optical properties. Our approach offers improved efficiency, versatility and scalability compared with previous approaches<sup>4–6</sup>.**

The intricate structures found on the wing scales of butterflies are difficult to copy, and it is particularly challenging to mimic the colour mixing effects displayed by *P. blumei* and *P. palinurus*<sup>7,8</sup>. The wing scales of these butterflies consist of regularly deformed multilayer stacks that are made from alternating layers of cuticle and air, and they create intense structural colours (Fig. 1). Although the *P. blumei* wing scales have previously been used as a template for atomic layer deposition (ALD)<sup>9</sup>, such an approach is not suitable for accurate replication of the internal multilayer structure on large surface areas.

The bright green coloured areas on *P. blumei* and *P. palinurus* wings result from a juxtaposition of blue and yellow-green light reflected from different microscopic regions on the wing scales. Light microscopy reveals that these regions are the centres (yellow) and edges (blue) of concavities that are 5–10  $\mu\text{m}$  wide, clad with a perforated cuticle multilayer<sup>7</sup> (Fig. 1d,e).

For normal light incidence, the cuticle–air multilayer shows a reflectance peak at a wavelength of  $\lambda_{\text{max}} = 525 \text{ nm}$ , which shifts to  $\lambda_{\text{max}} = 477 \text{ nm}$  for light incident at an angle of  $45^\circ$ . Light from the centre of the cavity is directly reflected, whereas retro-reflection of light incident onto the concavity edges occurs by double reflection off the cavity multilayer (Fig. 1g). This double reflection induces a geometrical polarization rotation<sup>10</sup>. If light that is polarized at an angle  $\psi$  to the initial plane of incidence is retro-reflected by the double bounce, it will pick up a polarization rotation of  $2\psi$  and the intensity distribution through collinear polarisers is therefore given by  $\cos^2(2\psi)$ . This leads to an interesting phenomenon: when placing the sample between crossed polarizers, light reflected off the centres of the cavities is suppressed, whereas retro-reflected light from four segments of the cavity edges is detected<sup>10,11</sup> (Fig. 1d, right).

In microstructures without this double reflection, both the colour mixing and polarization conversion are absent. This is the case for

scales of *P. ulysses*, a relative of *P. blumei* and *P. palinurus*, which have considerably shallower concavities<sup>8</sup> that cannot retro-reflect incident light, and thus show only a more conventional shimmering blue/violet colour.

The replication of natural photonic structures is useful for the creation of model systems to better understand structural colour in nature. Here, we demonstrate the replication of the periodically shaped multilayer structure of the *Papilio* butterfly scale in only five steps (Fig. 2). Avoiding the full structural complexity based on alternating solid cuticle and cuticle-pillar-supported air layers, we aim primarily to reproduce its optical characteristics. The multilayer structure of the artificial mimic is instead made from two solid inorganic constituents, which results in a much simpler structural design. However, with the appropriate materials, it is possible to fabricate structurally simplified replicas with authentic optical performance.

To create regularly arranged concavities of appropriate dimensions, polystyrene colloids with a diameter of 5  $\mu\text{m}$  were assembled on a gold-coated silicon substrate. A 2.5- $\mu\text{m}$ -thick layer of platinum or gold was then electrochemically grown into the interstitial space between the colloids, creating a negative replica<sup>12–14</sup>. Ultrasonication of the sample in dimethylformamide or acetone removed the colloids, resulting in a template of hexagonally arranged metal concavities. A  $\sim 20\text{-nm}$ -thick carbon film was sputtered onto the gold surface. Finally, a conformal multilayer of thin quarter-wave titania and alumina films was grown by ALD<sup>15</sup>. The carbon layer between the gold (or platinum) and the multilayer stack adsorbs light passing through the multilayer stack, reducing specular reflections and unwanted destructive interferences that would otherwise severely limit the optical performance.

Optical analysis of the natural butterfly structure and the artificial mimic was performed using a micro-spectroscopic set-up that allowed the collection of spectral data in a sample region less than 1  $\mu\text{m}$  in diameter. The two-dimensional translation of the sample under the objective of the microscope enabled acquisition of spectral maps across several concavities.

The artificial mimic presented in this work was composed of multilayer concavities  $\sim 4.5 \mu\text{m}$  in diameter and  $\sim 2.3 \mu\text{m}$  in height (Fig. 3a,b). The multilayer consisted of 11 alternating  $(57 \pm 4)\text{-nm}$ -thick titania and  $(82 \pm 4)\text{-nm}$ -thick alumina layers. These particular layer thicknesses were chosen in an attempt to create a quarter-wave stack with a stop-band centre wavelength in the green-yellow spectral range ( $\sim 550 \text{ nm}$ ) to match the reflectance band of the natural *Papilio* structure closely. The refractive indices of the titania ( $n_{\text{TiO}_2} = 2.5 \pm 0.1$ ) and alumina ( $n_{\text{Al}_2\text{O}_3} = 1.7 \pm 0.1$ ) layers were measured by ellipsometry. Neither material shows significant optical adsorption in thin films. The peak reflectance wavelength of the multilayer at  $\sim 550 \text{ nm}$  normal light incidence (that is,

<sup>1</sup>Department of Physics, Cavendish Laboratory, University of Cambridge, Cambridge CB3 0HE, UK, <sup>2</sup>Nanoscience Centre, University of Cambridge, Cambridge CB3 0FF, UK, <sup>3</sup>School of Physics, University of Exeter, Stocker Road, Exeter EX4 4QL, UK. \*e-mail: jjb12@cam.ac.uk; u.steiner@phy.cam.ac.uk

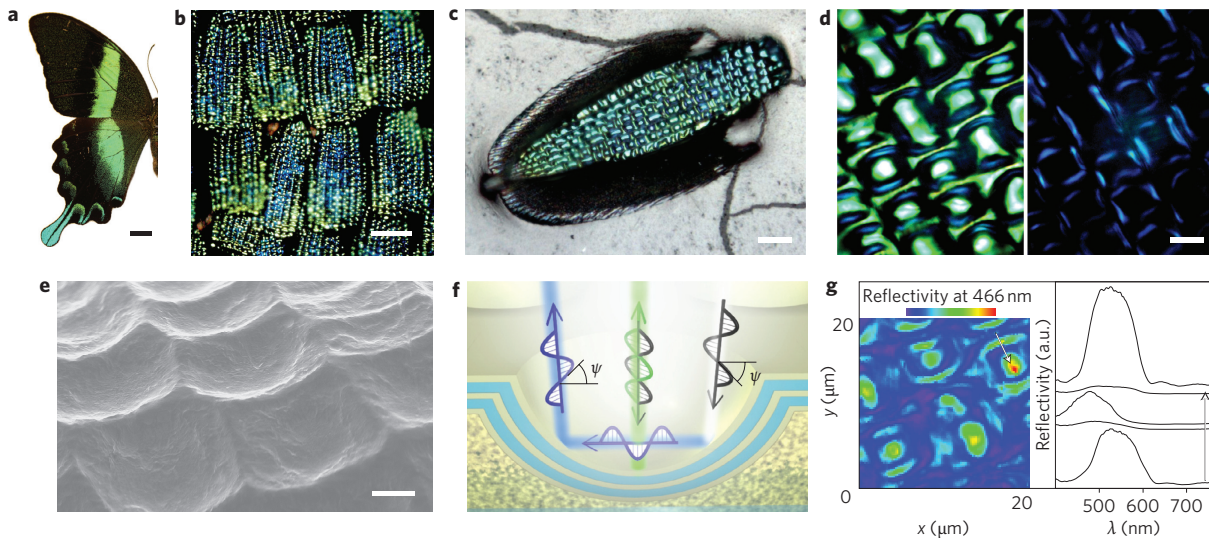


**Figure 1 | Natural photonic structure.** **a,b**, The bright green wings of the *P. blumei* butterfly result from the mixing of the different colours of light that are reflected from different regions of the scales found on the wings of these butterflies<sup>7</sup> (scale bars: **a**, 1 cm; **b**, 100  $\mu\text{m}$ ). **c**, *P. blumei* has two types of scales. The first type provides the colour and the second type, lying under the first, absorbs the transmitted light, preventing it from being back-scattered and thus assuring the purity of the reflected colours (scale bar: 20  $\mu\text{m}$ ). **d,e**, Optical micrographs (**d**, scale bar: 5  $\mu\text{m}$ ) and scanning electron micrograph (**e**, scale bar: 2  $\mu\text{m}$ ) showing that the surface of a wing scale is covered with concavities (diameter  $\approx$  5–10  $\mu\text{m}$ ) that are arranged in ordered lines along the scale. These concavities are clad with a multilayer that reflects yellow-green light at their centres and blue at their edges<sup>7</sup> (**d**, left). By observing the scales in an optical microscope with crossed polarizers, the yellow-green light is extinguished, but the blue light can still be detected along four segments of each edge (**d**, right). **f**, This effect is a result of a polarization rotation caused by a double reflection inside the concavity (which results partly from the out-of-plane reflections at each interface geometrically rotating the polarized light by an angle of  $2\psi$  (ref. 10)). **g**, Spectral maps of some of the concavities (left) confirm the optical anisotropy of the scale surface for unpolarized light. Spectra (right) taken at different positions along the white arrow in the spectral map show the shift in reflectance peak from green at the very edge of the concavity to blue close to the perimeter, and back to green at the centre.

in the centres of the cavity) corresponds well with theoretical predictions. Eleven layers are sufficient to achieve a peak reflectivity of more than 95%. These multilayer coated structures immediately display iridescent colours (Fig. 3c,d).

The bandwidth of the butterfly scale reflectance peak  $\Delta\lambda \approx 105$  nm is slightly larger than expected for a flat multilayer  $\Delta\lambda_{\text{th}} = (2/\pi)\lambda(\Delta n/\bar{n}) \approx 74$  nm, where  $\lambda$  is the peak-centre wavelength,  $\Delta n$  the refractive index difference, and  $\bar{n}$  the average refractive index of the multilayer materials. For the original butterfly structure, the refractive index of the solid cuticle layers is taken as  $n_{\text{cuticle}} = 1.56$  (ref. 11). A fit to the reflection data yields a refractive index of  $\sim 1.25$  for the cuticle-pillar-supported air layers. In comparison, the reflectance peak width of the artificial structure  $\Delta\lambda \approx 140$  nm ( $\Delta\lambda_{\text{th}} = 134$  nm) is broader because of the higher ratio  $\Delta n/\bar{n}$  of  $\text{TiO}_2$  and  $\text{Al}_2\text{O}_3$ .

Optical microscopy images show similar colour variations from the concavity centres to their edges for both the natural structure and the replica (compare Fig. 3e and Fig. 1d). This is confirmed by the peak shift in the corresponding spectra (Fig. 3g, left). The experimental data are well described by results of theoretical modelling of the multilayer structure. The anisotropic reflectance of the sample is clearly visible in the spectral maps (Fig. 3f, left).

The observation of the artificial mimic between crossed polarizers leads to a similar effect as described above for the butterfly structure. Only light incident onto four segments of the concavity edges is detected. The local surface normal of  $\sim 45^\circ$  gives rise to a double reflection at opposing cavity walls, causing a polarization rotation (Fig. 3f, right). As expected, this light is blueshifted with respect to the light reflected from the centres of the concavities. The artificial mimic therefore displays the same optical characteristics as the natural *P. blumei* wing scale structure.

In addition, a new feature arises from the double reflection of a high-refractive-index contrast dielectric stack: the two-peak reflectivity seen in Fig. 3 when the sample is placed between crossed

polarizers. The origin of this spectrum goes beyond the purely geometrical polarization conversion and depends on the different complex reflection coefficients  $r_s$  and  $r_p$  for *s*- and *p*-polarized light reflected from the multilayer. Both the magnitude and phase of  $r_s$  and  $r_p$  differ at different wavelengths relative to the reflection stop-band, with a spectrally narrower stop-band for *p*-polarized light. Full modelling of the multibounce reflectivity shows that the double bounce cannot produce a double-peak feature. However, retroreflection by means of a triple bounce can also occur<sup>10</sup> when light hits the outer edge of a concavity at an angle of  $\sim 60^\circ$ . For this triple bounce, the combination of geometrical polarization, relative-phase-shift-induced ellipticity and polarization conversion based on a reflectivity difference leads to the observed double-peak structure. The reflection data are well fit by superposition of reflections from both double and triple bounces (red curves in Fig. 3g, right). Although the triple-bounce reflection can also take place in natural *Papilio* scale concavities, the double-peak feature is not experimentally discernible for two reasons. First, optical modelling shows only a shallow dip in the triple-bounce reflection peak for the butterfly's air-cuticle multilayer concavities. Second, naturally occurring variations in concavity size and orientation lead to a mixing of the triple- and double-bounce signal, shadowing the faint double-peak feature entirely.

The angular change in peak reflectance wavelength  $\lambda$  follows the simple relation

$$m \frac{\lambda}{2} = d_1 \sqrt{n_1^2 - \sin^2 \theta_0} + d_2 \sqrt{n_2^2 - \sin^2 \theta_0} \quad (1)$$

where  $n_1$ ,  $n_2$ ,  $d_1$  and  $d_2$  denote the refractive indices and thicknesses of the two different multilayer materials,  $\theta_0$  is the light incidence angle and  $m$  is a positive integer. Using titania–alumina multilayers, peak wavelength shifts from the  $45^\circ$  double reflection of 35 nm can

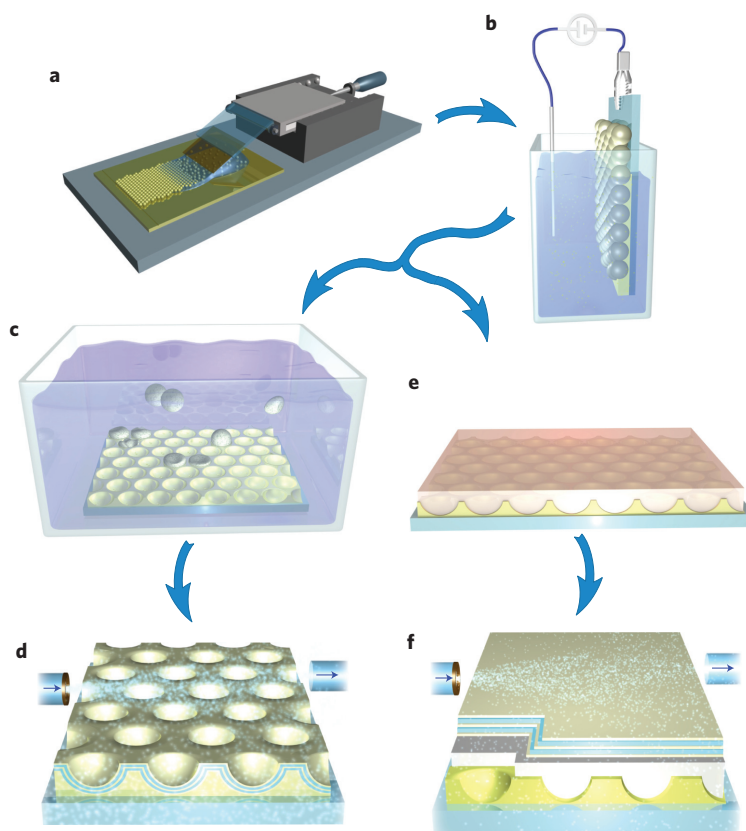


**Figure 2 | Sample fabrication.** **a**, Deposition of polystyrene colloids on a gold-coated silicon substrate. **b**, Growth of platinum or gold in the interstices of the colloidal array by electro-plating. The metal deposition is terminated when the thickness of the deposited film equals the microsphere radius. **c**, Removal of the polystyrene spheres from the substrate by ultrasonication in acetone. **d**, Sputtering of a thin carbon film and ALD of a stack of 11 alternating  $\text{TiO}_2$  and  $\text{Al}_2\text{O}_3$  layers (arrows indicate the precursor gas flow). **e, f**, In a second route, the colloids are molten to cover the cavities with a homogeneous film (**e**) which is covered by a  $\text{TiO}_2$ - $\text{Al}_2\text{O}_3$  multilayer (**f**).

be achieved, which compares with 60 nm for the natural butterfly structure. The use of a material with a smaller refractive index  $n < n_{\text{Al}_2\text{O}_3}$  for the low-refractive-index component in the multilayer stack will increase this peak wavelength shift.

Alternatively, using a combination of high-refractive-index dielectrics with lower refractive index contrast (for instance zinc oxide and titanium oxide,  $\Delta n/\bar{n} \approx 0.19$  as opposed to  $\Delta n/\bar{n} \approx 0.39$  for  $\text{Al}_2\text{O}_3$  and  $\text{TiO}_2$ ) for the multilayer coating would result in smaller reflectance band widths and consequently cause a more perceivable colour hue change across the concavities. However, high reflectivity with materials of low refractive index contrast requires Bragg mirrors with a larger number of layers.

We instead introduce a third alternative for the enhancement of a structural colour effect. A small simplification in the manufacture strategy described above leads to a pronounced colour variation (Fig. 4). Starting from a self-organized colloidal monolayer and electrochemical gold deposition, a multilayer is deposited. However instead of removing the colloids before ALD, the sample is annealed at 200 °C, and the colloids melt and form a continuous film of polymer, entirely filling and covering the concavities, thereby creating a flat surface. The ALD deposition of a planar titania–alumina multilayer on top of the polymer film results in a sample with periodically shaped resonant cavities. When seen in specular reflection the surface appears bright blue. Observed in back-reflection for non-normal light incidence it is strikingly red.

Visual information can be encoded into this photonic structure by photolithographically creating an arbitrary pattern in a ~200-nm-thick resist layer on the conducting surface before deposition of the colloidal template. The thin photoresist pattern does not

influence the assembly of the colloids but prevents gold electro-deposition. Consequently, the concave micro-mirrors are formed only in resist-free areas, thereby creating a picture, the colour of which varies dramatically with observation and light incidence angle.

The modified photonic structure has an optical signature that is very similar to that of Fig. 3 in terms of optical anisotropy when scanning across the concavities and the behaviour in polarized light. The important difference when compared to the conformal multilayer concavities is that the two predominant colours that are reflected on the microscale are not correlated by equation (1). The underlying mechanism for colour creation is different. While most of the incident light with wavelengths in the blue part of the visible spectrum is directly reflected by the upper multilayer and therefore does not enter the polymer cavity, light in the red part of the spectrum is transmitted by the multilayer and enters the cavities. There, most of it is reflected back in the direction of incidence by the underlying array of concave gold micro-mirrors. As expected, a blueshift in the reflection band of the multilayer is observed for increasing incidence angles, resulting in a variation of the back-reflected colour from red to orange. Only a small fraction of red light is scattered from the inter-cavity ridges into a wide angular range.

Additional cavity resonances in the red, particularly for light reflected off the concavity centres or the interstitial regions between adjacent concavities, contribute to the colour signature of the patterned device by a subtle modification in colour hue. For the thicker concavity centres, these resonances are closely spaced in wavelength compared to the interstitial regions. The experimentally observed spectra match well with theoretical models for layer

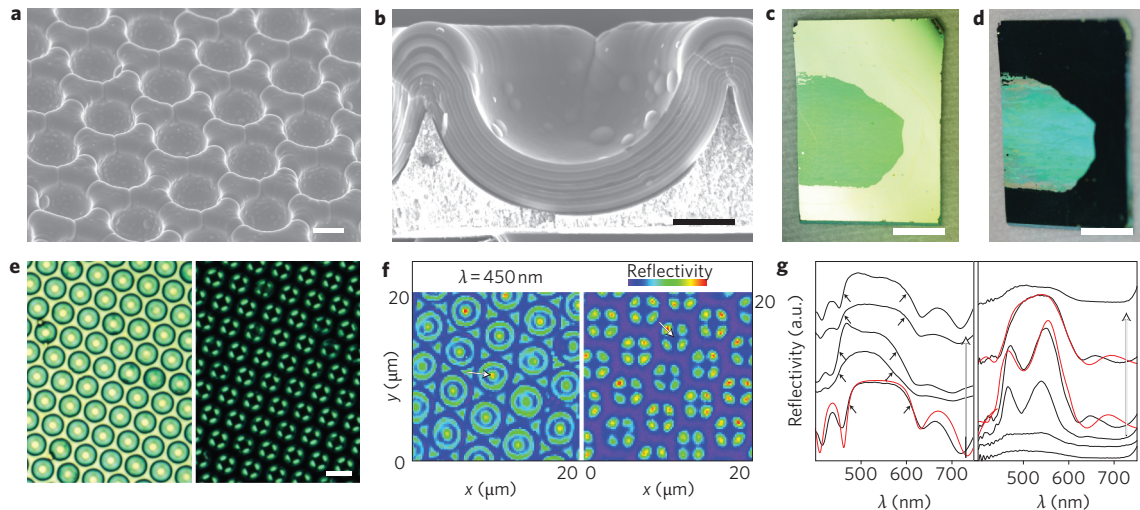


**Figure 3 | An artificial optical mimic.** **a,b**, SEM images of concavities covered by a conformal multilayer stack of 11 alternating layers of titania and alumina: top view (**a**, scale bar: 2  $\mu\text{m}$ ); cross-section (**b**, scale bar: 1  $\mu\text{m}$ ). **c,d**, With perpendicular light incidence the artificial replica appears green (**c**), but it reflects blue at grazing incidence (**d**), showing some iridescence (scale bars, 5 mm). **e**, Under a light microscope, the concavity edges appear turquoise, and the centres and interstitial regions are yellow (left). Between crossed polarizers only the green concavity edges are visible (right, scale bar, 5  $\mu\text{m}$ ). **f**, Spectral maps for  $\lambda = 450$  nm visualize the anisotropic reflectivity of the concavities for unpolarized light (left) and between crossed polarizers (right). **g**, Reflectivity along the paths indicated by arrows in the two frames in **f**, respectively. Left: The reflectance peak-shift across the concavities is clearly visible. The small arrows indicate the reflectance band edges. The red curve represents the predicted reflectance of the multilayer for normal light incidence. Right: light transmitted through crossed polarizers has undergone a polarization rotation by means of a double or triple bounce. The double bounce results in a single reflection peak and a triple bounce induces a double-peak feature. The red curves model the reflection as a superposition of double and triple bounce.

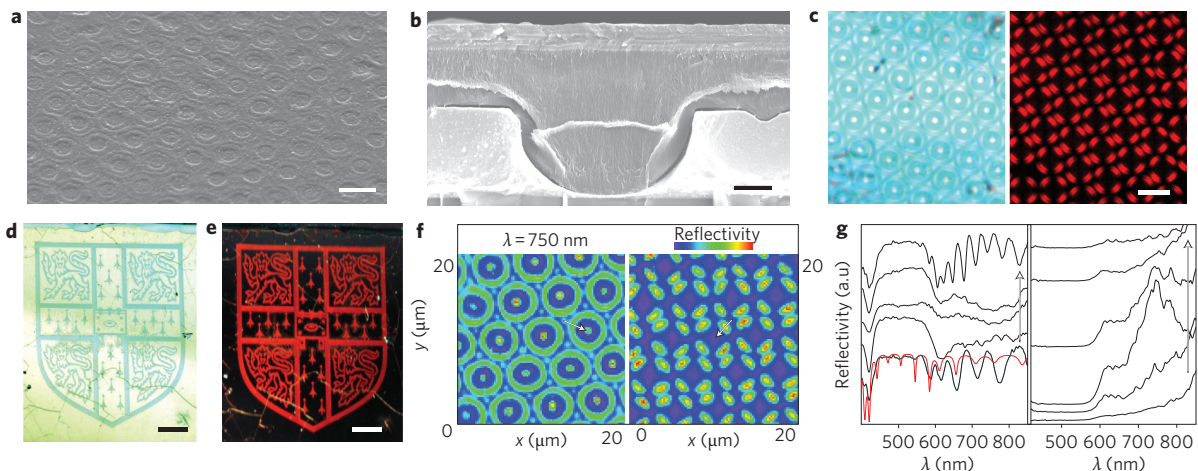


**Figure 4 | Modified mimic with enhanced optical performance.** **a,b**, SEM images of melted colloidal spheres embedded in 5- $\mu\text{m}$ -wide gold concavities and covered by a planar multilayer stack of 11 alternating layers of titania and alumina: top view (**a**, scale bar: 5  $\mu\text{m}$ ); cross-section (**b**, scale bar: 1  $\mu\text{m}$ ). **c**, Under unpolarized light, the edges of the concavities appear blue, while the centres and interstitial regions are reflecting in a broad spectral range (left). Between crossed polarizers only reflected red light is detected (right; scale bar 2  $\mu\text{m}$ ). **d,e**, Samples viewed in direct specular reflection (**d**) and in retro-reflection (**e**) (scale bars 5 mm), show a striking change in colour from blue to red. **f**, The anisotropic concavity reflectivity is clearly visible in the spectral maps for unpolarized  $\lambda = 750$  nm illumination (left) and between crossed polarizers (right). **g**, Spectra from distinct points on these spectral maps along the white arrows in **f**. Left: change in unpolarized reflectivity varying from the concavity border to its centre. The red line shows the calculated reflectance curve of the multilayer structure for the interstitial areas. The reflectance peak resulting from the multilayer does not shift significantly across the cavity, but strong resonances in the red are observed in the concavity centres and in the interstitial areas. Right: concavity reflectivity between crossed polarizers. Only red light retro-reflected from the inclined edges accompanied by a polarization rotation is detected.

thicknesses of  $\sim 3,850$  nm in the concavity centres and 1,865 nm in the interstitial regions (Fig. 4g).

The sample of Fig. 4 exhibits a pronounced variation from pale blue in specular reflection via red in all other directions to a particularly brilliant red in retro-reflection. By changing the multilayer spacing, it is possible to tune the colour seen in specular reflection across the whole visible range, accompanied by the complementary

colour in retro-reflection. A change in thickness of the polymer cavity results in a variation of the resonant wavelengths of the light that is transmitted through the top multilayer, modifying the colour seen in back-reflection for non-normal light incidence.

In summary, the intricate surface structure of *Papilio* butterflies was replicated in five simple steps by replicating a colloidal monolayer into an inorganic optical structure. A variation of concavity

height gives rise to a colour appearance mimicking either the single-coloured *P. ulysses* (suppressing double and triple bounce when the concavity walls are low enough) or the colour mixing of *P. palinurus* or *P. blumei*<sup>8</sup>. Square-centimetre-sized samples were fabricated in a facile and scaleable process. The manufactured mimics differ in important ways from the natural counterparts. First, they make use of solid inorganic materials instead of perforated cuticle lamella, the optical structure is much less fragile, and a much wider range in refractive index contrast can be achieved. Second, the in-plane hexagonal symmetry of the concavities (in contrast to the quasi-one-dimensional alignment of the concavities of a *Papilio* wing scale) can give rise to additional grating interferences, the extent of which can be controlled by varying the conditions under which the colloidal monolayer is deposited. Furthermore, we have demonstrated that a small variation of the natural design principle allows the creation of a striking colour separation effect. Rather than the juxtaposition of two colours in *Papilio* butterflies, adjustable switching for any colour and its complementary hue can be achieved. Square-centimetre-sized patterns and pictures with microscale resolution were encoded in the photonic structure, rendering this approach versatile for applications in the fields of security labelling or the manufacture of dynamic and vivid paints and coatings. This striking effect may also be used as a signalling cue in other patterned insects and should be a focus of future work.

Received 9 February 2010; accepted 20 April 2010;  
published online 30 May 2010

## References

- Vukusic, P. & Sambles, J. R. Photonic structures in biology. *Nature* **424**, 852–855 (2003).
- Land, M. F. The physics and biology of animal reflectors. *Prog. Biophys. Mol. Biol.* **24**, 75–106 (1972).
- Doucet, S. & Meadows, M. Iridescence: A functional perspective. *J. R. Soc. Interface* **6**, S115–S132 (2009).
- Parker, A. R. & Townley, H. E. Biomimetics of photonic nanostructures. *Nature Nanotech* **2**, 347–353 (2007).
- Watanabe, K., Hoshino, T., Kanda, K., Haruyama, Y. & Matsui, S. Brilliant blue observation from a *Morpho*-butterfly-scale quasi-structure. *Jpn J. Appl. Phys.* **44**, L48–L50 (2005).
- Huang, J., Wang, X. & Wang, Z. L. Controlled replication of butterfly wings for achieving tunable photonic properties. *Nano Lett.* **6**, 2325–2331, (2006).
- Vukusic, P., Sambles, R. J. & Lawrence, C. R. Colour mixing in wing scales of a butterfly. *Nature* **404**, 457 (2000).
- Vukusic, P., Sambles, R. J., Lawrence, C. R. & Wakely, G. Sculpted-multilayer optical effects in two species of *Papilio* butterfly. *Appl. Opt.* **40**, 1116–1125 (2001).
- Gaillot, D. P. *et al.* Composite organic-inorganic butterfly scales: production of photonic structures with atomic layer deposition. *Phys. Rev. E* **78**, 031922 (2008).
- Coyle, S., Prakash, G. V., Baumberg, J. J., Abdelsalam, M. & Bartlett, P. N. Spherical micro-mirrors from templated self-assembly: geometric reflectivity on the micron scale. *Appl. Phys. Lett.* **83**, 767–769 (2003).
- Vukusic, P., Sambles, J. R., Lawrence, C. R. & Wootton, R. J. Quantified interference and diffraction in single *Morpho* butterfly scales. *Proc. R. Soc. Lond. B* **266**, 1403–1411 (1999).
- Bartlett, P. N., Birkin, P. R. & Ghanem, M. A. Electrochemical deposition of macroporous platinum, palladium and cobalt films using polystyrene latex sphere templates. *Chem. Commun.* 1671–1672 (2000).
- Braun, P. V. & Wiltzius, P. Macroporous materials—electrochemically grown photonic crystals. *Curr. Opin. Colloid Interface Sci.* **7**, 116–123 (2002).
- Wijnhoven, J. E. G. J. *et al.* Electrochemical assembly of ordered macropores in gold. *Adv. Mater.* **12**, 888–890 (2000).
- Puurunen, R. L. Surface chemistry of atomic layer deposition: a case study for the trimethylaluminum/water process. *J. Appl. Phys.* **97**, 121301 (2005).

## Acknowledgements

The authors acknowledge financial support from the EPSRC (EP/G060649/1, EP/E040241, EP/C511786/1). M.K. acknowledges support from DAAD (German Academic Exchange Service) and the Cambridge Newton Trust.

## Author contributions

P.V. and M.K. performed the studies of the natural photonic structure. M.K., M.S., P.S. and U.S. conceived and designed the artificial mimics. M.S. provided the colloidal templates. P.S. and S.M. performed the electro-deposition. P.S. produced the photolithographic resist pattern for the modified mimic. M.K. and P.S. realized the atomic layer deposition. M.K. characterized the optical performance and the topology of the samples. F.H. and J.B. provided the algorithms necessary to perform the optical measurements and to create the spectral maps. M.K., J.B., U.S. and P.V. analysed the data. M.K., U.S. and J.B. wrote the paper. All authors discussed the results and commented on the manuscript.

## Additional information

The authors declare no competing financial interests. Reprints and permission information is available online at <http://npg.nature.com/reprintsandpermissions/>. Correspondence and requests for materials should be addressed to J.J.B. and U.S.